

The Wilson–Bappu Effect: a tool to determine stellar distances.

G. Pace^{1,2}, L. Pasquini², and S. Ortolani³

¹ Dipartimento di Astronomia, Università di Trieste, Via G.B. Tiepolo 11, 34131 Trieste, Italy

² European Southern Observatory, Karl Schwarzschild Strasse 2, 85748, Garching bei München, Germany

³ Dipartimento di Astronomia, Università di Padova, Vicolo dell'Osservatorio 5, 35122 Padova, Italy

Received July 15, 2002; accepted July 16, 2002

Abstract. Wilson & Bappu (1957) have shown the existence of a remarkable correlation between the width of the emission in the core of the K line of Ca II and the absolute visual magnitude of late-type stars.

Here we present a new calibration of the Wilson–Bappu effect based on a sample of 119 nearby stars. We use, for the first time, width measurements based on high resolution and high signal to noise ratio CCD spectra and absolute visual magnitudes from the *Hipparcos* database.

Our primary goal is to investigate the possibility of using the Wilson–Bappu effect to determine accurate distances to single stars and groups.

The result of our calibration fitting of the Wilson–Bappu relationship is $M_V = 33.2 - 18.0 \cdot \log W_0$, and the determination seems free of systematic effects. The root mean square error of the fitting is 0.6 magnitudes. This error is mostly accounted for by measurement errors and intrinsic variability of W_0 , but in addition a possible dependence on the metallicity is found, which becomes clearly noticeable for metallicities below $[\text{Fe}/\text{H}] \sim -0.4$. This detection is possible because in our sample $[\text{Fe}/\text{H}]$ ranges from -1.5 to 0.4.

The Wilson–Bappu effect can be used confidently for all metallicities not lower than ~ -0.4 , including the LMC. While it does not provide accurate distances to single stars, it is a useful tool to determine accurate distances to clusters and aggregates, where a sufficient number of stars can be observed.

We apply the Wilson–Bappu effect to published data of the open cluster M67; the retrieved distance modulus is of 9.65 magnitude, in very good agreement with the best distance estimations for this cluster, based on main sequence fitting.

Key words. Stars: Wilson–Bappu effect, Chromospheric emission, Ca II K–line

1. Introduction

The K line of Ca II is the deepest and widest absorption line in the spectra of the late type stars, and its core shows the characteristic double reversal profile: an emission with a central self-absorption (see e.g. Pasquini et al. 1988).

Since the discovery by Wilson & Bappu (1957) of the existence of a linear relationship between the logarithm of the width of the Ca II emission (W_0) and the stellar absolute visual magnitude (the so called Wilson–Bappu effect), several calibrations of this effect have been attempted. However the Wilson–Bappu relationship (WBR) has only seldom been used to determine stellar distances to single stars or aggregates.

The reliability of past calibrations of the WBR has been limited by the lack of two crucial elements:

1. Precise and accurate parallaxes for nearby stars;
2. High quality data and objective method of measuring W_0 .

The first point has been overcome by Wallerstein et al. (1999), who produced a new calibration by exploiting the *Hipparcos* database. This work however was hampered by the fact that it was still based on W_0 measurements

* Observations collected at ESO, La Silla

Send offprint requests to: L. Pasquini, e-mail: lpasquin@eso.org

provided by Wilson (1967, 1976), performed on photographic plates. For our calibration we have used W_0 measurements performed on new, high quality CCD spectra, so that also the second point has been, for the first time, properly accounted for.

A new, reliable WBR determination is especially interesting since new detectors and state of the art spectrographs can now produce excellent CaII data even for stars in stellar clusters and associations as distant as several kiloparsecs. For these clusters and associations, we could therefore apply the WBR to derive their distance. This possible application is the main ground of our effort to retrieve a reliable calibration for the WBR.

2. Data sample and observations

The full sample for which spectra have been collected (data shown in Table 1) consists of 152 stars, but the present study is limited to stars with relative parallax errors smaller than 10%. We have also excluded from the original sample known multiple systems. After this trimming, the final sample includes 119 stars.

All the stars but the Sun are included in the *Hipparcos* catalogue, from which trigonometric parallaxes and visual magnitudes have been taken.

The absolute visual magnitude of the Sun has been taken from Hayes (1985) The sample has been selected in order to span a wide range of luminosities (from $M_V \simeq -5$ to $M_V \simeq 9$).

The observations were obtained between November 1988 and September 1996, at ESO, La Silla, with the Coudé Echelle Spectrometer, at the focus of the Coudé Auxiliary Telescope. The resolution is $R=60000$ and the S/N ratio ranges from $\simeq 30$ to $\simeq 100$ at the bottom of the line (for more details about the first spectra see Pasquini (1992)).

For ~ 30 stars, multiple spectra were taken, and for the Sun 9 spectra are available.

Spectral types and metallicities were obtained from the Cayrel de Strobel et al. (1997) catalogue. For the stars not included in this catalogue, spectral types are taken from the *Hipparcos* database. The projected rotation velocities are from Głęboczi et al. (2000).

3. Measurements and calibration

W_0 was measured manually on all of the spectra. We have also developed an IDL macro which performs a multi Gaussian fitting to the K–line double–reversal profile, but it has not been used for the final computation because it has proven quite fragile for the correct determination of the broad line absorption profile. We are working on improving the method, and we may report further progress elsewhere.

W_0 has been computed as the difference in wavelength between the two points taken at the intensity equal to the average between those of the K1 minimum and K2 peak on either side of the emission profile (see Figure 2).

We found that the definition of W_0 which we have adopted correlates better with M_V than two other widths also measured:

- the difference in wavelength between K1 minima;
- the width taken at the intensity equal to the average between those of the K1 minima and K2 maxima.

No correction for instrumental broadening was applied to W_0 . The reason is explained in Sect.5.4.

We notice that our definition of W_0 differs slightly from others used in the literature. Wilson & Bappu (1957) define W as the difference in wavelength between the red edge and the violet edge of the emission profile. They apply to the measured value in the spectra a linear correction: $W_0 = W - 15 \text{ km} \cdot \text{s}^{-1}$. Wilson (1959) kept the original definition but applied a revised correction: $18 \text{ km} \cdot \text{s}^{-1}$ instead of 15. Lutz (1970) introduced a new definition of W_0 , defining it as the width at half of the maximum of the emission profile. Lutz’s definition is very similar to ours with the exception that we found the our definition easier to use in case of difficult spectra and more robust (see below).

W_0 measurements are subject, of course, to measurement errors. For each star we have computed an accuracy qualifier, ΔW_0 , in the following way. For the stars with two or more spectra available we derived it as the half of the difference between the largest and smallest measured widths. For stars with only one available spectrum, we measured W_0 with multiple methods, and took the difference between the extrema of the measurements. Then we added quadratically to this value (which in some cases was 0) that of the Sun (0.030 \AA), whose W_0 measurements variations are supposed to be caused only by the intrinsic variation of the line width and by the limit of the resolution power of the spectrograph. We have used ΔW_0 as an estimate of the mean error in W_0 . The standard error of $\log W_0$ (where W_0 is in $\text{km} \cdot \text{s}^{-1}$) for each star, is retrieved applying the propagation of the mean error.

Independent of the signal to noise ratio, for some stars it is intrinsically more difficult to measure W_0 . This is because their spectra show asymmetric self absorption, either produced by interstellar lines or by blueshifted winds or cosmic rays. Inactive, low luminosity stars will typically show shallow reversals, which are more difficult to measure.

Some of the most doubtful examples and difficult cases are presented in Figure 1, in order to make the reader acquainted with the spectra and the possible error sources. In some cases, when strong blending was present or the

profile was highly asymmetric, we have measured W_0 by doubling the value measured for the “clean” half of the line. Anyway, the majority of the spectra we dealt with were as good as the one showed in Figure 2.

We have also computed the standard error on the absolute magnitude of each star. This error has two components: the mean error on the apparent visual magnitude (which is, in most of the cases, negligible) and the error given by the uncertainty in the parallax, which has to be computed via the propagation of the error.

The fit of the WBR was performed by means of the IDL routine “fitexy”, which implements the algorithm described in Press et al. (1989). The algorithm fits a straight line to a set of data points by taking into accounts errors on both coordinates.

We repeated the solution by rejecting stars not passing 3σ -, 2.5σ - or 2σ -criteria. The results so obtained are presented in Table 2

It is fundamental to note that, independent of the different sigma clipping criterion used, the solutions found are extremely stable, giving the same fit to within 1σ .

We adopt in the following: $M_V = 33.2 - 18.0 \cdot \log W_0$ (W_0 is in $\text{km} \cdot \text{s}^{-1}$) obtained rejecting HD 63077 and HD 211998, with a standard deviation: $\sigma_{WBR} = 0.6$ mag. The two rejected stars are the most metal poor of the sample, which we will argue in Sect. 5.5 is the most likely cause of their large residuals.

Hereafter we indicate with $M_V(K)$ the value of M_V derived for a single star from its W_0 via the WBR. In Figure 5 the $\log W_0$ vs M_V diagram is shown, with the error bars representing standard errors in both coordinates. The calibration line retrieved is also plotted.

4. Comparison with other results

In order to evaluate the external robustness of the relationship, a comparison with other independent investigations is fundamental. Many attempts in the past 40 years have been made to calibrate the WBR based on ground-based trigonometric parallaxes (Wilson 1959; Hodge & Wallerstein 1966; Lutz & Kelker 1975; Głębocki & Stawikowski 1978). Wallerstein et al. (1999) (hereafter WMPG) used a very large sample of stars with *Hipparcos* parallaxes and relative measurement errors smaller than 20%. As already stated, their work is based on the width measurements available in the literature, mostly from Wilson (1967, 1976), which suffer from low spectral accuracy.

We note here that such measurements are based on the definition of W given in Wilson & Bappu (1957), corrected for instrumental broadening as in Wilson (1959) (see Sect. 3). So the quantity W_0 which they adopt is not exactly the same as ours, although the two quantities are expected to be strongly correlated.

WMPG used a linear least squares fitting both not weighted and weighted only in absolute magnitude with $\frac{\epsilon_{\pi}}{\pi}$. As WMPG advised, using weighted least squares means giving more weight to the lowest part of the diagram, containing the dwarfs that are, on the average, much closer, and therefore with smaller measurement errors on parallaxes. Using the weight for both the coordinates, as we did, does not produce to the same effect, because at the same time the dwarfs have also smaller W_0 , and so larger relative measurement errors, i.e. larger standard errors for $\log W_0$. In Figure 6 we show the comparison of our calibration and the weighted calibration of WMPG.

We think that this comparison is a strong test of the reliability of the WBR. In fact, with the only exception of having used *Hipparcos* parallaxes, the two samples are independent: less than the 40% of the stars we used in the computation are common to WMPG. Different stars means different distributions in magnitudes, metallicities and effective temperatures. Furthermore, different spectrographs were used, different measurements (even based on different definitions of W_0) were performed as well as a different analysis. Taken at the face values, our calibration and WMPG’s one are in good agreement for all stars brighter than $M_V \sim 2$, while for dwarfs, the discrepancy is stronger, reaching a difference of 1.5 magnitudes at $M_V \sim 9$.

In order to investigate how much of this discrepancy is due to the differences in W_0 measurements, we compared, for the 64 stars common to the two data sets, the W_0 measurements of WMPG and ours. Actually 20 of these stars are among the 33 not used in our WBR computation, but for the present comparison this is irrelevant. The two sets of measurements show, as expected, a very strong linear correlation: the slope of the $W_{0_{our}}$ vs $W_{0_{WMPG}}$ linear fitting is very much closed to unity: 1.003, with an intercept of $-5.34 \text{ km} \cdot \text{s}^{-1}$ (see Figure 7).

If we subtract $5.34 \text{ km} \cdot \text{s}^{-1}$ to our W_0 measurements, we obtain a data set homogeneous to that of WMPG, and performing the fitting with the new values gives following WBR: $M_V = 29.7 - 16.3 \cdot \log W_0$. This result matches very well that of WMPG, as it can be seen from Figure 6. We conclude that the reliability of the WBR is excellent, and that the only reason for the discrepancy between the calibrations is the difference in the definition of W_0 .

On the other hand we notice that care is needed in measuring W_0 : its definition, and possibly the resolution of the spectra used should be the same as those of the calibration adopted.

The fact that the difference between our and WMPG’s measurements is about $5 \text{ km} \cdot \text{s}^{-1}$, quite similar to the projected slit width for $R=60000$, could suggest that the instrumental profile should indeed be linearly subtracted by our W_0 measurements to obtain an-instrument free calibration.

We do not believe that this is the case, because:

1. Other studies (Lutz 1970) have shown as the case of linear subtraction of instrumental profile is not the best choice.
2. Our observations of one star (HD 36069) taken at different resolutions to estimate this effect show that the variations observed in W_0 measurements are not better accounted for by a linear subtraction of the instrumental profile, as shown from the measurements in Table 3.

For sake of completeness, we remind that the WBR is also valid for the k–line of the Mg II, and that the best calibration to date is the one of Cassatella et al. (2001), which also uses *Hipparcos* data and IUE spectra. Their result is: $M_V = 34.56 - 16.75 \cdot \log W_0$

5. Is the WBR a good distance indicator?

The spread around the WBR is still too large to consider it as a reliable distance indicator for single stars. The question we are now going to investigate in this section is if the WBR is suitable to determine the distance of clusters of stars. A necessary condition which such clusters have to satisfy is, of course, that for a sufficient number of members, a high quality spectrum, showing a clear double reversal profile of the K–line, is available.

The possibility of using the WBR to determine accurate cluster distances is strictly related to the causes of the scatter: whether or not it is due to entirely random errors or systematic effects. Among the possible causes of scatter, we mention:

- random effects:
 - measurement errors,
 - cyclic variation in the chromospheric activity,
 - variability of some of the stars of the sample;
- systematic effects:
 - reddening,
 - instrumental effects,
 - Lutz–Kelker effect (hereafter LKE),
 - hidden parameters, i.e. parameters other than W_0 and M_V on which the WBR could depend.

White & Livingston (1981) observed the chromospheric emission of the K line of the sun during a whole solar cycle. They found a maximum variation of $\log W_0$ of about 0.05 during such a period. If we assume that most of the stars are affected by a variation of $\log W_0$ of the same order of magnitude, the amount of scatter introduced by the cyclic variation of the chromospheric activity would represent a relevant fraction of the spread observed in the data. Nevertheless, this variability cannot fully explain the observed root mean square error of the WBR fitting. With typical uncertainties in W_0 due to measurement errors and natural variations of the stellar line width of about 0.036 Å (cf. Table 1), this error, for stars with intermediate widths, say $W_0 = 0.8$ Å, accounts for about 0.35 mag of $\sigma_{WBR} = 0.6$ mag. Therefore, it is necessary to investigate further reasons of uncertainty in the determination of the WBR.

Among possible causes of biases we should consider reddening, the LKE (Lutz & Kelker (1973), hereafter LKP), instrumental effects and the presence of multiple systems.

5.1. Lutz–Kelker effect

The LKE is the bias due to the fact that a symmetric error interval $[\pi - \sigma_\pi, \pi + \sigma_\pi]$ around the estimated parallax π , does not correspond to a symmetric error interval in distances around $\frac{1}{\pi}$. The inner spherical corona centred in the Sun having radii $\frac{1}{\pi + \sigma_\pi}$ and $\frac{1}{\pi}$, has a volume smaller than the outer spherical corona. So, assuming a homogeneous space density for the stars, we expect that, for a fixed measured parallax, stars having a true distance greater than $\frac{1}{\pi}$, i.e. those in the outer corona, will outnumber the stars having a distance smaller than $\frac{1}{\pi}$. There is therefore a systematic trend to underestimate distances. The correction which has to be applied to each star, has been calculated in LKP. It depends only on the relative error $\frac{\sigma_\pi}{\pi}$.

Our sample has been selected to include only stars with $(\frac{\sigma_\pi}{\pi} \leq 0.1)$. Furthermore, out of the 119 stars, only 7 have $\frac{\sigma_\pi}{\pi}$ exceeding 0.075. For these values the LKE is negligible compared with other errors involved: 0.06 mag for $\frac{\sigma_\pi}{\pi} = 0.075$ and 0.11 mag for $\frac{\sigma_\pi}{\pi} = 0.1$ (See Table 1 in LKP)

5.2. Reddening

We have assumed that all stars have zero reddening. This assumption is justified by the fact that the sample stars are all within ~ 200 parsec.

The most distant star, HD 43455, has a distance of 205 pc, and it is the only one for which we were not able to find out a secure upper limit to the reddening.

HD 78647 has a distance of 176 pc, and a galactic latitude lower than 7.6° , so we can get a rough estimation of its

reddening on the Neckel & Klare’s maps (Neckel et al. 1980). For this star, A_V does not exceed ~ 0.1 mag.

The remaining stars are within 107 pc. According to Sfeir et al. (1999) (see their Figure 2) the upper limit of the equivalent width of the D2 Na I line for such a distance is 200 mÅ. From this quantity we can get the Hydrogen column density (Welsh et al. 1994): $N(\text{HI}) \sim 2 \cdot 10^{20}$, which yields a colour excess: $E_{B-V} \sim 0.03$, or an upper limit for A_V of about 0.1 mag.

Furthermore, 100 of the 119 stars in this sample, are within 75 parsec, so they are in the so called Local Bubble (see e.g. Sfeir et al. 1999), and they are not affected by detectable extinction.

5.3. Multiple systems

The presence of unrecognised multiple systems in the sample, gives rise to a systematic underestimation of $M_V(K)$, because we could associate the width of the K line emission of one component to the magnitude of the whole system. To avoid this effect, we checked all the objects of our sample on the SIMBAD database and we have excluded all the known multiple systems.

5.4. Instrumental effects

The measured W_0 is likely larger than the intrinsic one because of the broadening introduced by the spectrograph. The larger the projected slit width is the stronger the instrumental broadening will be. We have shown in Sect. 4, by means of data in Table 3, that a linear correction for instrumental broadening (i.e. subtracting the projected slit width from W_0) would not be appropriate. Similar results were found by Lutz (1970), who concluded that a quadratical correction should be used. To minimize this effect, our calibration is based on high resolution spectra (the projected slit width is about 0.066 Å or $5 \text{ km} \cdot \text{s}^{-1}$), and applying a quadratical correction even to the smallest W_0 value (that of HD 42581, 0.30 Å) we would obtain: $W_0 - W_{0\text{corrected}} = W_0 - \sqrt{W_0^2 - (0.066)^2} = 0.0074 \text{ Å}$, well below its estimated measurement error, i.e. $\Delta W_0 = 0.02 \text{ Å}$. For larger values of W_0 , $W_0 - W_{0\text{corrected}}$ is even smaller. Hence, the quadratical correction is negligible for all stars in our sample. We believe that the quadratical correction is more appropriate than the linear one, and it should be applied when dealing with low resolution spectra, but it is not certain that such a small adjustment would represent a real improvement when dealing with data of resolution comparable to that used in this work.

5.5. Other causes

Many authors searched for additional parameters on which the WBR could depend, finding contradictory results. Głębocki & Stawikowski (1978) proposed a corrected WBR with a term for the intensity of the emission that WMPG have rejected.

Parsons (2001), analysing the calibration of WMPG, suggested a trend for high luminosity stars that our data seem not to confirm: he suggested that $O - C$ (i.e. the difference between the absolute magnitude from *Hipparcos* parallax and the one retrieved by means of the WBR) increases with increasing T_{eff} for spectral types earlier than $\sim K3$, while the opposite is true for the other stars. He also concludes that this trend gets stronger for brighter stars. According to Figure 3, while we can draw no conclusions for late type stars, our data seem to suggest a trend opposite to that proposed by Parsons (2001) for spectral types earlier than $\sim K3$.

The most obvious hidden parameter to search for is projected rotational velocity. High rotational velocity can influence W_0 in several ways, either because fast rotating stars will tend to be more active (see e.g. Cutispoto et al. 2002), or because the width of the line core may be modified by the higher rotational velocity (see e.g. Pasquini et al. 1989). We have 53 stars for which $V \cdot \sin i$ is available, and none are really fast rotators, only for one object $V \cdot \sin i$ exceeds $10 \text{ km} \cdot \text{s}^{-1}$. Our conclusion is that, among slow rotators, there is hardly any dependence of the residuals on $V \cdot \sin i$: we find a correlation coefficient of 0.12

We have finally searched for a dependence of the $O - C$ on metallicity. Such a dependence can also be expected, considering that in stars having lower abundances the core of the line may sample different layers of the atmosphere.

In particular we have checked whether the WBR is still valid for very metal poor stars. Figure 4 shows two $O - C$ vs $[\text{Fe}/\text{H}]$ diagrams: the one on the left refers to all the stars with available metallicities, in the other diagram only stars with $[\text{Fe}/\text{H}] < -0.3$ are plotted. A weak but not negligible dependence of the WBR on metallicity does exist, and it gets much stronger for metal poor stars. The correlation coefficient is 0.64, and it becomes 0.82 when the 19 most metal poor stars are considered, as shown on the right panel of figure 4.

19 stars are too few to obtain any firm quantitative conclusions. In particular, the $O - C$ vs $[\text{Fe}/\text{H}]$ relationship, to which they would point out (the straight line in right panel of Figure 4), should be further investigated by means

of a richer sample. The existence of such a relationship for metal poor stars has been independently suggested by Dupree & Smith (1995), who studied 53 metal poor giants, none of which is in our sample.

We think that the WBR should be applied very carefully to very metal poor stars (e.g. stars more metal poor than $[\text{Fe}/\text{H}] \sim -0.4$) and that further metal poor calibrators should be observed before applying it to very metal poor clusters.

6. Application to M67

After deriving the WBR, and showing that the scatter is mostly due to random errors, we have the opportunity to test it on a group of stars belonging to a well studied open cluster. M67 CaII spectra were published by Dupree et al. (1999) (See Figure 2, 3 and 4 therein) for 15 stars on the RGB and clump region, and they are suitable for our analysis of the WBR. Andrea Dupree kindly provided us with all the spectra in digital form.

Since M67 has been extensively studied, the retrieved distance modulus can be compared with values obtained from other authors. Carraro et al. (1996) provide a detailed study of M67. They derive, on the basis of the Colour Magnitude Diagram, $9.55 \leq (m - M)_V \leq 9.65$ mag.

Montgomery et al. (1993) performed a photometric survey of the central region of M67. They compared their photometry with two theoretical isochrones to retrieve distance modulus and age for M67. From $V, B - V$ CMDs, they found $(m - M)_V = 9.60$ for both isochrones (but different ages were found), they have also used a $V, V - I$ CMD, giving $(m - M)_V = 9.85$. Dinescu et al. (1995) found $9.7 \leq (m - M)_V \leq 9.8$ mag, obtained by letting E_{B-V} varying between its upper (0.06 mag) and lower (0.03 mag) limits. Their isochrones were constructed using model atmospheres with new opacities. In Montgomery et al. (1993) other results from the literature are reported, ranging from 9.55 to 9.61.

In summary, all distance modulus determinations for M67 are in the range $9.55 \leq (m - M)_V \leq 9.85$ mag.

M67 is a solar metallicity cluster, so we do not need to take care of the metallicity effect which may affect the WBR. The W_0 measurements were performed in the same way as for the calibration stars, and the results are given in Table 4. Out of the 15 stars of the original sample we have selected a subsample of 10, which suitable spectra were available, either for quality or clearness of the core reversal. In fact some of the spectra do not show a clear unambiguously recognisable double reversal feature, so that the measurement is unreliable. We did not use the stars with the following Sanders ID numbers (Sanders 1977) : 258, 989, 1074, 1316, 1279. Even among the 10 selected stars some show a clearer profile than others, and for four of them the measurements were more uncertain (of the order of 0.1 Å) and they have been flagged with an asterisk in Table 4.

We have to consider that M67 spectra were acquired for other purposes, and in particular they have lower resolution and lower S/N ratio than the typical calibration spectra, so we expect a standard error on the single measurement higher than the σ_{WBR} derived above.

In Table 4 the distance modulus determinations for the single stars retrieved by means of the WBR are given. They range from 8.1 to 10.9 mag. The mean value is ~ 9.7 In spite of the poorer quality of the spectra, all the deviation can be explained on the base of the intrinsic spread around the WBR.

For sake of accuracy we have also taken into account the effect of the difference in resolution between the calibration spectra and the M67 observations (5 and 11 $\text{km} \cdot \text{s}^{-1}$ respectively). A simple, quadratic correction for the difference between the two projected slit widths is applied in the sixth column of Table 4. The correction does not change the result in an appreciable way.

When considering all stars a simple mean gives $(M-m) = 9.61$ mag; which becomes 9.65 when discarding the 4 most uncertain measurements.

We expect that the standard error in our determination of the distance of M 67 would be about: $\frac{\sigma_{WBR}}{\sqrt{6}} \sim 0.3$ if we used 6 spectra of quality similar to those used for our calibration ($\sigma'_{M67} \sim 0.2$ if we had 10 spectra of the same quality).

Trying to push further this application would definitely represent a gross over interpretation of the data, however we find it extremely interesting and encouraging that a simple application, using published data, can provide a distance modulus in the range between 9.5 and 9.8, in excellent agreement with completely independent measurements, such as those obtained with main sequence model fitting.

7. Conclusions

We have shown that the coupling of CCD high resolution, high S/N ratio data with the use of the *Hipparcos* parallaxes allows a good determination of the WBR. The root mean square error found around this relationship (0.6 magnitude) is not good enough to determine accurate distances to single stars, but it can be used to infer accurate distances of clusters or groups, provided that they are not too metal poor. This is possible because the uncertainties in the relationship are mostly due to random errors (measurements, cycles) and not from systematic effects. This implies that once one has observed a sufficient number of stars, n , the distance modulus standard error can be reduced to about

$0.6\text{mag}/\sqrt{n}$. Its extension to metal poor objects (e.g. stars with $\text{Fe}/\text{H} < -0.4$) would require extra care to fully evaluate the impact of low metallicity on the relationship. When using our WBR in photometric parallax determinations, the resolution used should be comparable (within a factor ~ 3) to that of the calibration ($R=60000$), to avoid large corrections, and care has to be exercised in measuring W_0 , following the proper calibration definition.

Acknowledgements. We are greatly indebted to P. Bristow and N. Bastian for their careful reading of the manuscript. We thank the referee, Elena Schilbach, for very valuable comments and suggestions, which improved considerably the quality of this paper. Special thanks to A. Dupree, who kindly provided us with the M67 spectra.

References

- Carraro, G., Girardi, L., Bressan A., & Chiosi, C. 1996, A&A 305, 849
 Cassatella, A., Altamore, A., Badiali, M., & Cardini, D. 2001, A&A 374, 1085
 Cayrel de Strobel, G., Soubiran, C., Friel, E.D., Ralite, N., & Francois P. 1997, A&AS 124, 229
 Cutispoto, G., Pastori, L., Pasquini, L., de Medeiros, J.R., Tagliaferri, G., & Andersen, J. 2002, A&A 384, 491
 Dinescu, D. I., Demarque, P., Guenther, D. B., & Pinsonneault, M. H. 1995, AJ109, 2090
 Dupree, A. K., & Smith, G. H. 1995, AJ 110, 405
 Dupree, A. K., Whitney, B. A., & Pasquini, L. 1999, ApJ 520, 751
 Hayes, D.S. 1985, IAU Symp. 111, 347
 Głębocki, R., & Stawikowski, A. 1978, A&A 68, 69
 Głębocki, R., Gnacinski, P., & Stawikowski, A. 2000, AcA 50, 509
 Hodge, P.W., & Wallerstein, G. 1966, PASP 78, 411
 Lutz, T.E., 1970, AJ 75, 1007
 Lutz, T.E., & Kelker, D.H. 1973, PASP 85, 573
 Lutz, T.E., & Kelker D.H. 1975, PASP 87, 617
 Montgomery, K. A., Marschall, L. A., & Janes, K. A. 1993, AJ 106, 181
 Neckel, Th., Klare, G., & Sarcander, M. 1980, A&AS 42, 251
 Parsons, S.B. 2001, PASP 113, 188
 Pasquini, L., Pallavicini, R., & Pakull, M. 1988, A&A 191, 253
 Pasquini, L., Pallavicini, R., & Dravins, D. 1989, A&A 213, 261
 Pasquini, L. 1992, A&A 266, 347
 Press, W.H., Teukolsky, S.A., Vetterling, V.T., & Flannery, B.P. 1992, Numerical Recipes (Cambridge Univ. Press), 660
 Sanders, W. L. 1977, A&AS 27, 89
 Sfeir, D. M., Lallement, R., Crifo, F., & Welsh, B. Y. 1999, A&A 346, 785
 Wallerstein, G., Machado–Pelaez, L., & Gonzalez, G. 1999, PASP 111, 335
 Welsh, B. Y., Craig, N., Vedder, P. W., & Vallerger, J. V. 1994, ApJ, 437, 638
 White, O.R., & Livingston, W. C. 1981, ApJ 249, 798
 Wilson, O.C., & Bappu, M.K.V. 1957, ApJ 125, 661
 Wilson, O.C. 1959, ApJ 130, 499
 Wilson, O.C. 1967, PASP 79, 46
 Wilson, O.C. 1976, ApJ 205, 823

Table 1: Our data sample. The full sample consists of 152 stars, 33 of which have not been used in the present study, because of their high measurement error in the parallax ($\frac{\sigma_\pi}{\pi} > 0.1$) or because they are multiple systems. We have flagged their HD identifiers with an asterisk. Column 1: HD ID number of the star. Column 2: W_0 in Å. Column 3: accuracy qualifier for W_0 , again in Å. Its mean value is 0.036. Column 4: absolute visual magnitude using *Hipparcos* parallaxes. For the Sun we used the value given by Hayes (1985). Column 5: spectral type from Cayrel De Strobel Catalogue. When the spectral type is not available from this catalogue the data is taken from the *Hipparcos* database, and is flagged with a dagger. Column 6: mean metallicity, when available from Cayrel De Strobel Catalogue. Column 7: projected rotation velocity, when available from Glębocki et al. (2000).

Star	W_0 [Å]	ΔW_0 [Å]	M_V	Sp.Type	[Fe/H]	$V \cdot \sin i$
SUN	0.49	0.030	4.82	G2V	0.00	1.6
HD 203244	0.47	0.030	5.42	G5V	-0.21	-
HD 17051	0.62	0.030	4.22	G0V	-0.04	5.7
HD 1273*	0.5	0.030	5.03	G2V †	-0.61	-
HD 20407	0.41	0.042	4.82	G1V	-0.55	-
HD 20766	0.50	0.030	5.11	G2.5V	-0.25	-
HD 20630	0.53	0.030	5.03	G5Vvar	0.11	4.6
HD 20807	0.44	0.036	4.83	G1V	-0.21	-
HD 20794	0.43	0.030	5.35	G8V	-0.38	-
HD 26491	0.50	0.058	4.54	G3V	-0.23	-
HD 1581	0.49	0.15	4.56	F9V	-0.20	3
HD 30495	0.55	0.030	4.87	G3V	0.11	3
HD 32778	0.42	0.030	5.28	G0V	-0.61	-
HD 34721	0.60	0.032	3.98	G0V	-0.25	-
HD 36435	0.48	0.030	5.53	G6–G8V	-0.02	4.5
HD 39587	0.56	0.030	4.70	G0V	0.08	9.3
HD 43834	0.51	0.036	5.05	G6V	0.01	1.8
HD 48938	0.53	0.042	4.31	G2V	-0.47	-
HD 3443	0.47	0.036	4.61	K1V	-0.16	2.7
HD 53705	0.60	0.036	4.51	G3V	-0.30	-
HD 3795	0.46	0.030	3.86	G3–G5V	-0.73	-
HD 63077	0.41	0.032	4.45	G0V	-0.90	-
HD 3823	0.60	0.042	3.86	G1V	-0.35	3
HD 64096*	0.50	0.030	4.05	G2V †	-	-
HD 65907	0.52	0.050	4.54	G0V	-0.36	-
HD 67458	0.47	0.036	4.76	G4IV–V	-0.24	-
HD 74772	0.89	0.032	-0.17	G5III	-0.03	5.8
HD 202457	0.61	0.036	4.13	G5V	-0.14	-
HD 202560	0.35	0.030	8.71	M1–M2V †	-	-
HD 202628	0.55	0.030	4.87	G2V	-0.14	-
HD 202940*	0.6	0.030	5.20	G5V	-0.38	1.2
HD 211415	0.48	0.032	4.69	G3V	-0.36	1.7
HD 211998	0.47	0.036	2.98	A3V	-1.50	-
HD 212330	0.51	0.067	3.75	G3IV	0.14	1.8
HD 212698	0.54	0.030	4.04	G3V	0.08	9.7
HD 14412	0.40	0.042	5.81	G5V	-0.53	-
HD 14802	0.62	0.032	3.48	G2V	0.10	3
HD 104304	0.55	0.036	4.99	G9IV	0.17	1.7
HD 114613	0.56	0.030	3.29	G3V †	-	2.7
HD 11695	1.02	0.030	-0.57	M4III †	-	-
HD 194640	0.46	0.032	5.17	G6–G8V †	-	-

Table 1 cont.

Star	W_0 [Å]	ΔW_0 [Å]	M_V	Sp.Type	[Fe/H]	$V \cdot \sin i$
HD 20610*	0.86	0.032	0.39	K0III	-0.07	-
HD 209100	0.39	0.030	6.89	K4.5V	0.14	0.7
HD 211038	0.56	0.032	3.64	K0–K1V	-	-
HD 219215	1.03	0.030	0.05	M2III †	-	-
HD 29503*	0.80	0.030	1.23	K0III	-0.11	-
HD 35162	0.86	0.042	0.28	G8–K0II–III	-0.31	-
HD 36079*	0.92	0.030	-0.63	G5II	-0.20	5.1
HD 4128	0.94	0.032	-0.30	K0III	-0.01	3.3
HD 43455	1.05	0.032	-1.55	M2.5III †	-	-
HD 4398	0.82	0.032	0.44	G8–K0III †	-	-
HD 102212	1.01	0.067	-0.87	M0III †	-	-
HD 111028	0.72	0.036	2.40	K1III–IV	-0.40	1.5
HD 112300	1.04	0.030	-0.57	M3III	-0.09	-
HD 113226	0.94	0.030	0.37	G8IIIvar	0.04	2.8
HD 114038	0.89	0.030	0.29	K1III	-0.04	-
HD 115202	0.66	0.030	2.26	K1III †	-	-
HD 115659	0.92	0.030	-0.04	G8III	-0.03	4.2
HD 117818	0.81	0.032	0.67	K0III	-0.40	-
HD 119149*	1.15	0.030	-0.70	M2III †	-	-
HD 120477	0.90	0.032	-0.33	K5.5IIIvar	-0.23	2.2
HD 121299	0.83	0.032	0.70	K2III	-0.03	-
HD 123123	0.83	0.030	0.79	K2III †	-0.05	-
HD 124294	0.95	0.030	0.00	K2.5IIIb	-0.45	-
HD 125454	0.82	0.030	0.52	G8III	-0.22	-
HD 126868	0.77	0.030	1.72	G2III †	-	14.3
HD 129312*	1.04	0.030	-1.37	G7IIvar	-0.30	6.5
HD 130952	0.88	0.030	0.82	G8III	-0.29	-
HD 133165	0.83	0.032	0.64	K0.5IIIb	-0.22	-
HD 136514	0.85	0.030	0.98	K3IIIvar	-0.14	0.6
HD 138716	0.68	0.032	2.30	K1IV	-0.13	2.5
HD 140573	0.88	0.030	0.87	K2IIIb	0.14	1.4
HD 141680	0.82	0.032	0.68	G8III	-0.28	1.1
HD 145001*	0.94	0.050	-0.37	G8III	-0.26	9.9
HD 145206*	1.00	0.032	-0.51	K4III	0.04	3.2
HD 146051	1.12	0.030	-0.85	M0.5III	0.32	-
HD 146791	0.83	0.030	0.64	G9.5IIIb	-0.13	-
HD 148349*	0.90	0.030	-0.71	M2 †	-	-
HD 148513*	1.10	0.036	-0.15	K4III	-0.14	0.6
HD 150416*	1.04	0.030	-0.48	G8II–III	+0.04	-
HD 151217	1.00	0.032	0.00	K5IIIvar	-0.11	2.3
HD 152334	0.98	0.030	0.30	K4III †	-	-
HD 152601	0.82	0.030	0.82	K2III	0.00	-
HD 161096	0.91	0.030	0.76	K2III	0.05	2.7
HD 164349*	1.17	0.030	-1.84	K0.5IIIb	-0.32	-
HD 165760	0.91	0.095	0.33	G8III	-0.15	2.2
HD 168723	0.67	0.030	1.84	K0III–IV	-0.10	2.6
HD 169156*	0.77	0.030	0.82	G9IIIb	-0.17	-
HD 169767	0.74	0.030	1.15	G8–K0III †	-	-
HD 170493	0.44	0.030	6.67	K3V †	-	3.5
HD 171443	0.98	0.030	0.21	K3III	0.09	1.8
HD 171967*	1.10	0.032	-1.57	M2III †	-	-
HD 173009*	1.11	0.032	-1.14	G8IIb	0.05	6.0
HD 173764*	1.80	0.036	-2.40	G4IIa	-0.15	6.5
HD 175775*	1.07	0.030	-1.76	G8–K0II–III	-0.19	-

Table 1 cont.

Star	W_0 [Å]	ΔW_0 [Å]	M_V	Sp.Type	[Fe/H]	$V \cdot \sin i$
HD 176678	0.84	0.032	0.73	K1IIIvar	-0.19	-
HD 177565	0.51	0.030	4.98	G5IV	0.03	-
HD 17970	0.44	0.050	6.01	K1V †	-	-
HD 181391*	0.77	0.030	1.61	G8III	-0.21	2.8
HD 182572	0.60	0.032	4.27	G8IV	0.38	2.3
HD 183630*	1.02	0.050	-0.90	M1IIIvar †	-	-
HD 184406	0.79	0.030	1.80	K3IIIb	0.05	1.3
HD 186791*	1.32	0.030	-3.02	K3II	0.00	3.5
HD 188310	0.91	0.032	0.73	G9IIIb	-0.32	2
HD 189319	1.13	0.030	-1.11	K5III †	-	-
HD 190248	0.54	0.030	4.62	G7IV	-0.26	-
HD 190406	0.49	0.030	4.56	G1V †	-	5
HD 191408	0.38	0.030	6.41	K2V †	-	0.1
HD 194013	0.75	0.032	0.91	G8III–IV	-0.03	1
HD 195135	0.88	0.036	1.07	K2III	0.03	-
HD 196574*	0.86	0.030	-1.04	G8III	-0.13	3.7
HD 196758	0.89	0.036	0.77	K1III	-0.12	1.8
HD 196761	0.42	0.030	5.53	G8–K0V †	-	-
HD 198026*	1.03	0.030	-1.24	M3IIIvar †	-	-
HD 201381	0.73	0.032	1.00	G8III	-0.15	2.8
HD 203504	0.86	0.030	0.71	K1III	-0.14	1.2
HD 205390	0.41	0.030	6.30	K2V †	-	-
HD 206067	0.87	0.032	0.76	K0III	-0.17	1
HD 206453	0.82	0.030	-0.03	G8III	-0.20	-
HD 206778*	1.78	0.030	-4.19	K2Ibvar	-0.05	6.5
HD 209747	1.06	0.030	0.32	K4III	0.00	2.3
HD 209750*	2.14	0.030	-3.88	G2Ib	0.18	6.7
HD 211931*	0.86	0.030	1.03	A1V †	-	-
HD 212943	0.78	0.030	1.33	K0III	-0.33	0.6
HD 213042	0.44	0.030	6.71	K4V †	-	-
HD 2151	0.62	0.030	3.45	G2IVvar	-0.18	3
HD 216032*	1.03	0.030	-1.28	K5II †	-	-
HD 217357	0.33	0.030	8.33	K5–M0V †	-	-
HD 21749	0.38	0.030	7.01	K5V †	-	-
HD 217580	0.45	0.036	6.34	K4V †	-	3.6
HD 218329	1.12	0.030	-0.43	M2III †	-	-
HD 220339	0.42	0.030	6.35	K2V †	-	5.5
HD 220954	0.86	0.030	0.83	K1III	-0.10	0.6
HD 27274	0.41	0.030	7.06	K5V †	-	-
HD 32450	0.33	0.030	8.66	M0V †	-	-
HD 42581	0.30	0.030	9.34	M1–M2V †	-	3
HD 4747	0.46	0.030	5.78	G8–K0V †	-	-
HD 56855*	1.76	0.030	-4.91	K3Ib †	-	-
HD 59717*	1.05	0.030	-0.50	K5III †	-	-
HD 68290*	0.84	0.030	0.95	K0III	-0.03	-
HD 73840*	1.01	0.030	-0.56	K3III	-0.21	-
HD 74918*	0.73	0.030	0.11	G8III	-0.20	-
HD 75691	0.96	0.030	-0.01	K3III	-0.11	-
HD 78647	1.65	0.030	-3.99	K4Ib–IIvar	0.23	8.9
HD 81101	0.82	0.030	0.62	G6III †	-	-
HD 82668	1.21	0.361	-1.15	K5III †	-	-
HD 85444	0.93	0.030	-0.50	G6–G8III	-0.14	2.9
HD 90432	1.04	0.030	-1.15	K4III	-0.12	-
HD 93813	0.96	0.030	-0.03	K0–K1II	-0.32	-

Table 1 cont.

Star	W_0 [Å]	ΔW_0 [Å]	M_V	Sp.Type	[Fe/H]	$V \cdot \sin i$
HD 95272	0.90	0.030	0.44	K1III	-0.15	-
HD 9540	0.50	0.030	5.52	K0V †	-	-
HD 98430	0.89	0.030	-0.31	K0III	-0.40	1.8

criterion	NUMBER OF STARS	NUMBER OF	FINAL RESULT		
	REJECTED	ITERATIONS	a	b	σ_{WBR}
3σ	2	2	33.2	-18.0	0.60
2.5σ	5	3	33.5	-18.3	0.56
2σ	16	9	33.6	-18.3	0.49
$\sigma_a = 0.5$ & $\sigma_b = 0.3$.					

Table 2. The resulting calibrations after three different sigma clipping criteria. σ_{WBR} is the the standard deviation of a single measurement. σ_a and σ_b are the standard deviations of the retrieved parameters, respectively, a and b of $M_V = a + b \cdot \log W_0$. The stability of the solution shows the reliability of the WBR as a distance indicator.

Resolution	W_0 [Å]	$W_{0_{incorr}}$ [Å]	$W_{0_{quadcorr}}$ [Å]
R=110000	0.923	0.887	0.922
R=80000	0.915	0.866	0.914
R=60000	0.925	0.859	0.923
R=60000	0.918	0.852	0.916
R=40000	0.929	0.831	0.924
R=30000	0.953	0.822	0.944
Variance	$1.8 \cdot 10^{-4}$	$5.6 \cdot 10^{-4}$	$1.2 \cdot 10^{-4}$

Table 3. Six W_0 measurements of HD 36079, made on spectra with different resolutions, both corrected and not corrected for instrumental broadening subtracting linearly the projected slit width. The variance of data in Column 3 data is about 3 times that of Column 1 and, most important, the corrected W_0 decreases with increasing correction. These measurements show that the linear subtraction of the instrumental profile is not appropriate for our data. A quadratic correction seems to be more justified for our data (see the last Column).

Column 1	Column 2	Column 3	Column 4	Column 5	Column 6
Sanders ID	W_0 (Å)	m _V	$M_V(K)$	(m-M) _V	(m-M) _V
			no corr	no corr	corr
S1010	0.851	10.48	0.657	9.823	9.742
S1016*	0.700	10.30	2.184	8.116	7.996
S1074*	0.784	10.59	1.298	9.292	9.196
S1135	0.963	9.37	-0.310	9.680	9.617
S1221	0.854	10.76	0.629	10.131	10.050
S1250*	0.997	9.69	-0.581	10.271	10.212
S1479	0.868	10.55	0.502	10.048	9.970
S1553	0.970	8.74	-0.366	9.106	9.044
S488	1.010	8.86	-0.682	9.542	9.485
S978*	1.080	9.72	-1.206	10.926	10.876
Mean value using all stars:				9.693	9.619
Mean value using only unflagged stars:				9.722	9.651

Table 4. Data about the sample of the 10 stars in M67. Column 1: Sanders ID number (Sanders 1977) of the star. The stars with doubtful measurements are flagged with an asterisk. Column 2: Wilson–Bappu width in Å. Column 3: apparent visual magnitude, from Table 1 in Dupree et al. (1999) (see references therein). Column 4: absolute magnitude inferred from the WBR. Column 5: retrieved distance modulus. Column 6: retrieved distance modulus using corrected widths: $W_{0_{corrected}} = \sqrt{W_0^2 - PSW_{R=30000}^2 + PSW_{R=60000}^2}$ (PSW is the projected slit width).

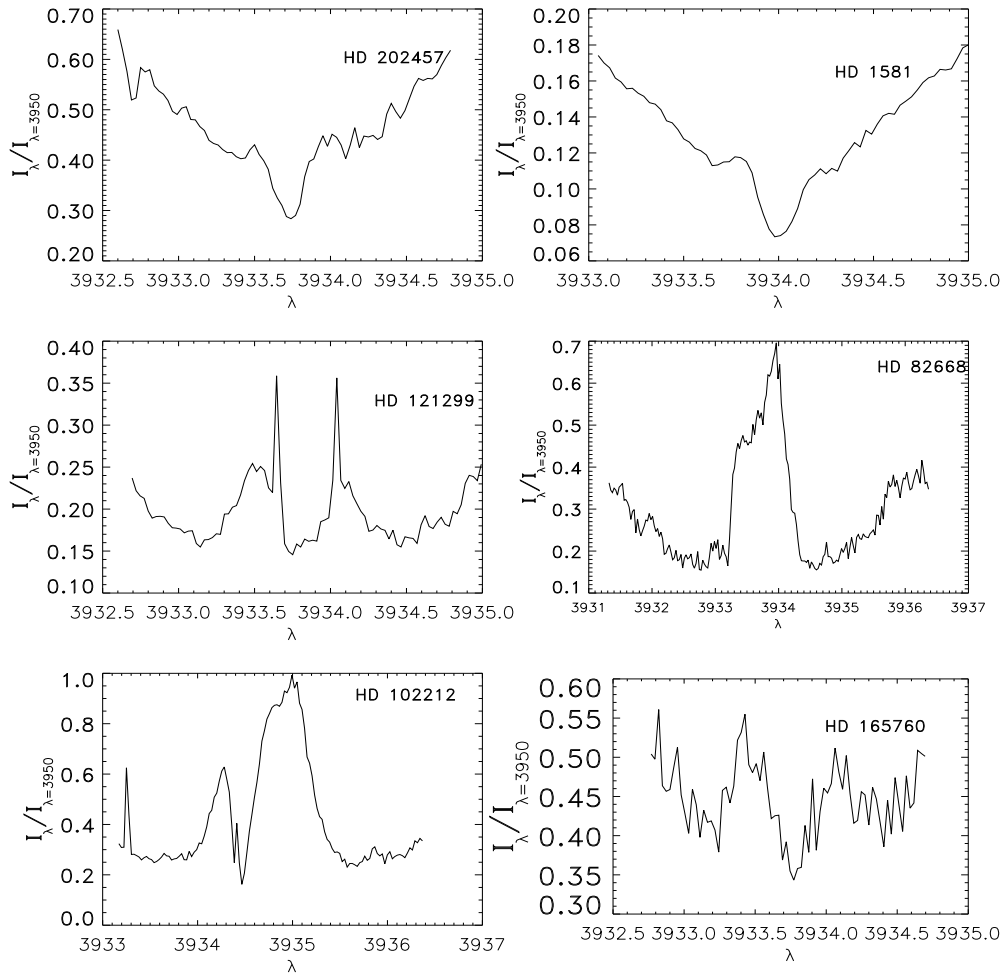


Fig. 1. Doubtful examples of Ca II K line profiles. The spectra are affected by cosmic rays, may be blended with interstellar absorption, which strongly influence the emission profile observed in HD 82668, or, as in the case of HD 102212, show a blueshifted wind. In other cases, such as in HD 1581, the emission is very weak.

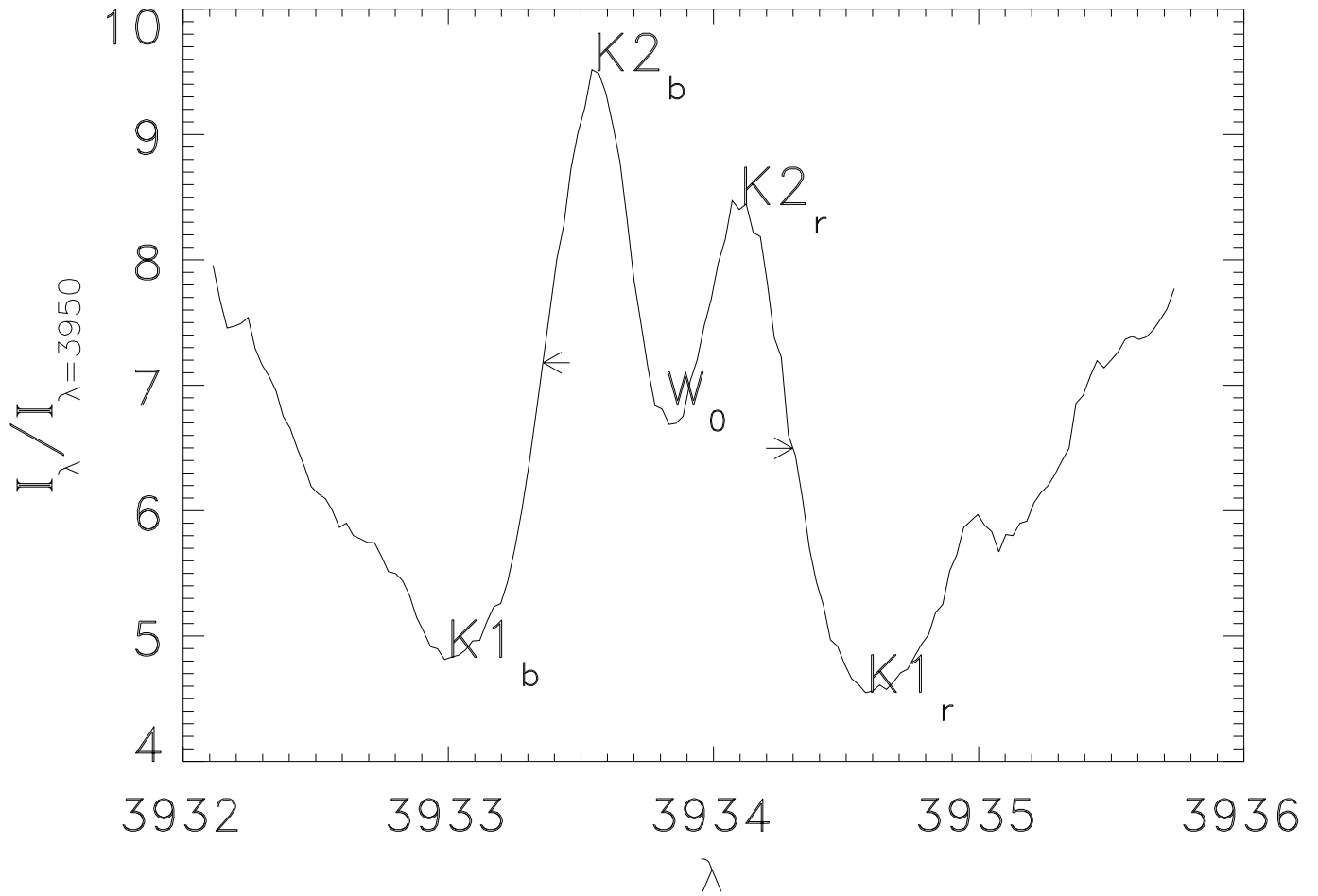


Fig. 2. Spectrum of HD 4128. Most of the spectra of our sample have a comparable quality.

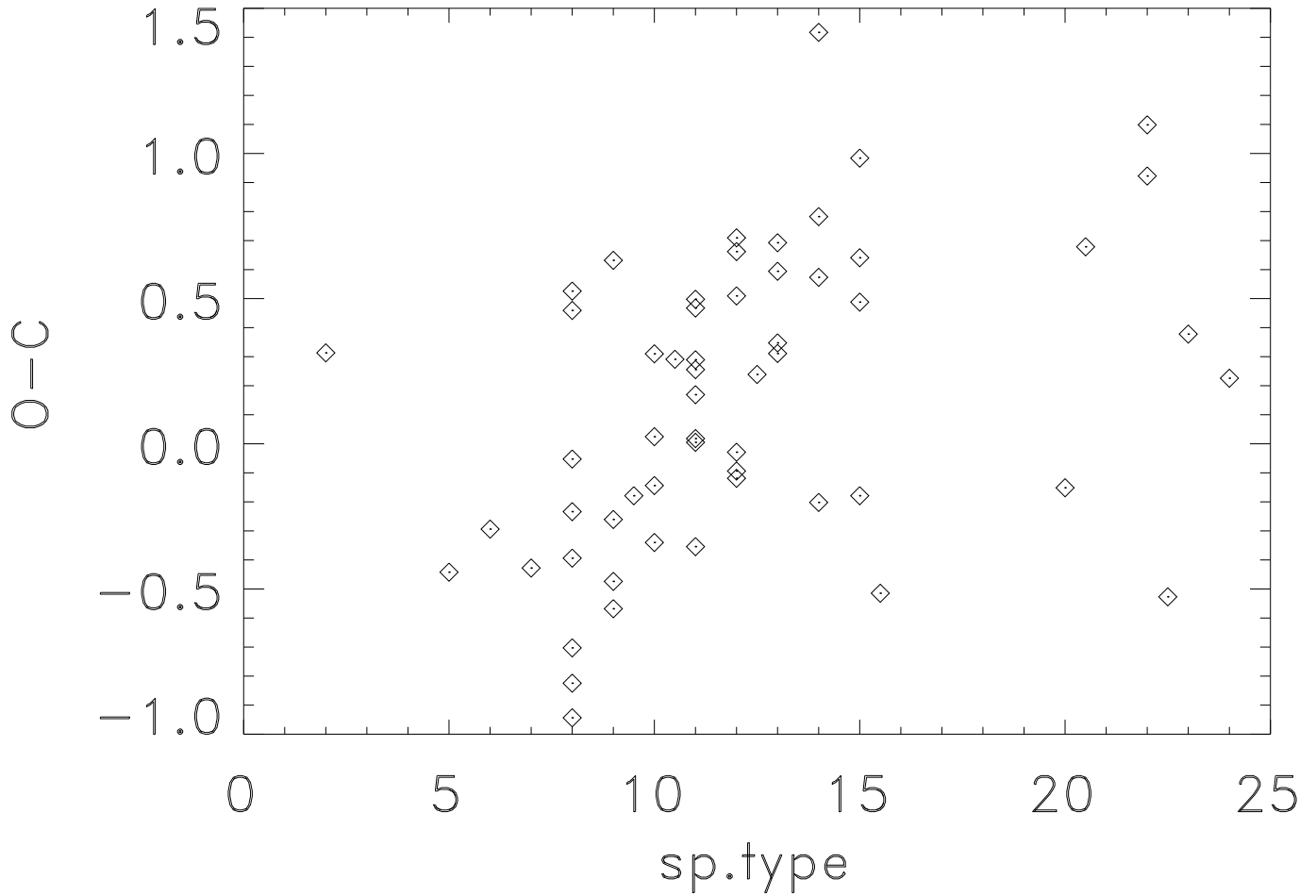


Fig. 3. The spectral type diagram vs $O - C$. The spectral types are indexed as in Parsons (2001): 0 is for G0 stars, 1 for G1 and so on. Only luminous stars are plotted (no IV and V luminosity classes).

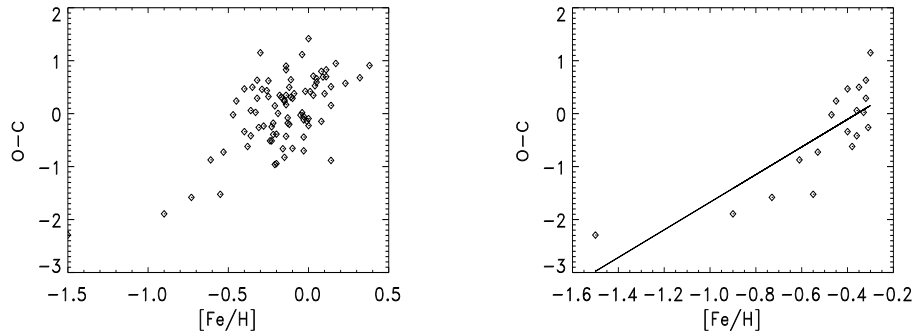


Fig. 4. The $O - C$ vs $[\text{Fe}/\text{H}]$ diagrams both for all stars of the sample with available metallicities (on the left) and for metal poor stars only. On the latter is also shown the retrieved regression line, which has a slope as high as 2.61.

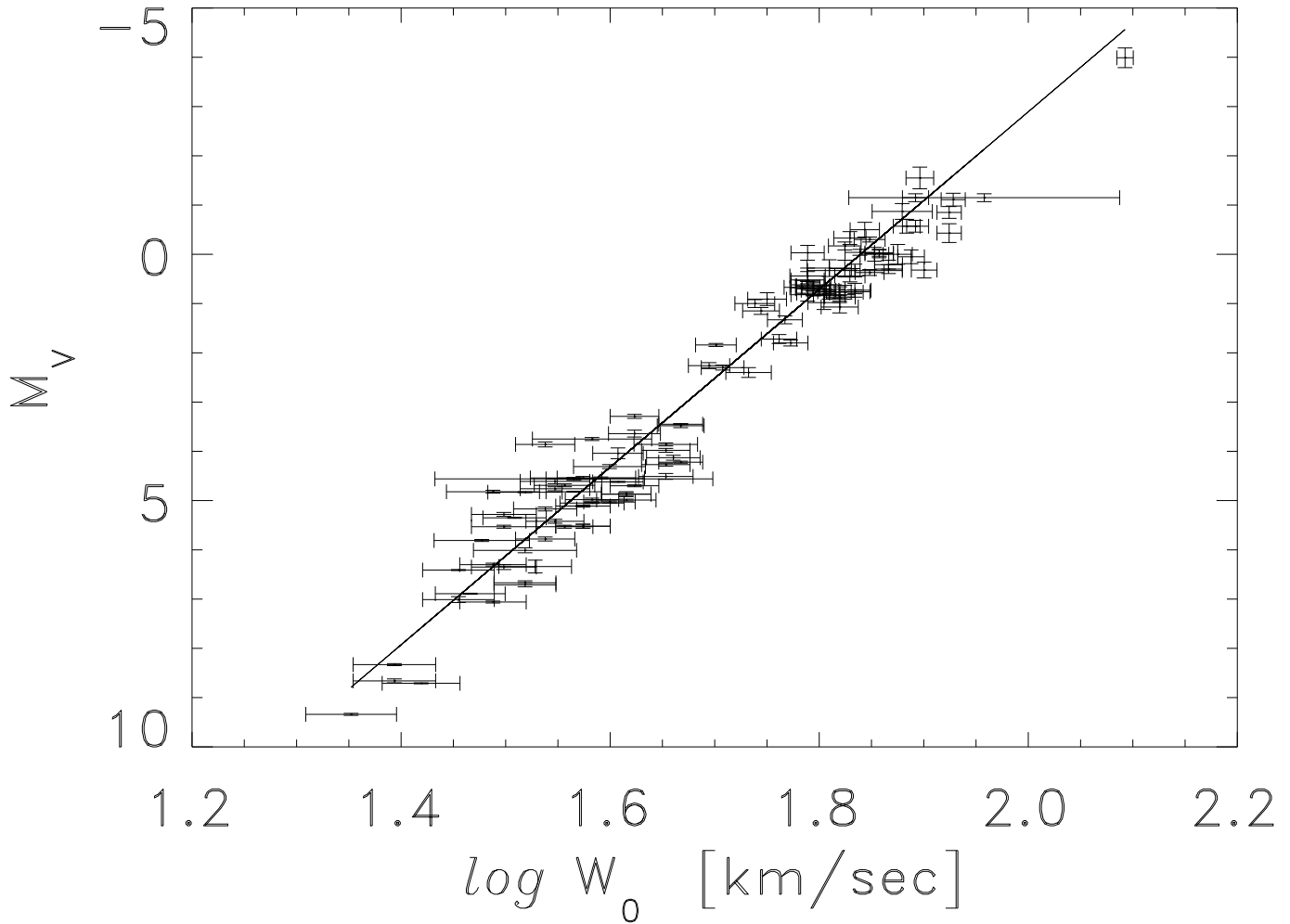


Fig. 5. Our calibration of the Wilson–Bappu Effect: $M_V = 33.2 - 18.0 \cdot \log W_0$. This calibration is the 3σ criterion one in Table 2 (HD 63077 and HD 211998 are not used). The error bars represent standard errors in both the coordinates.

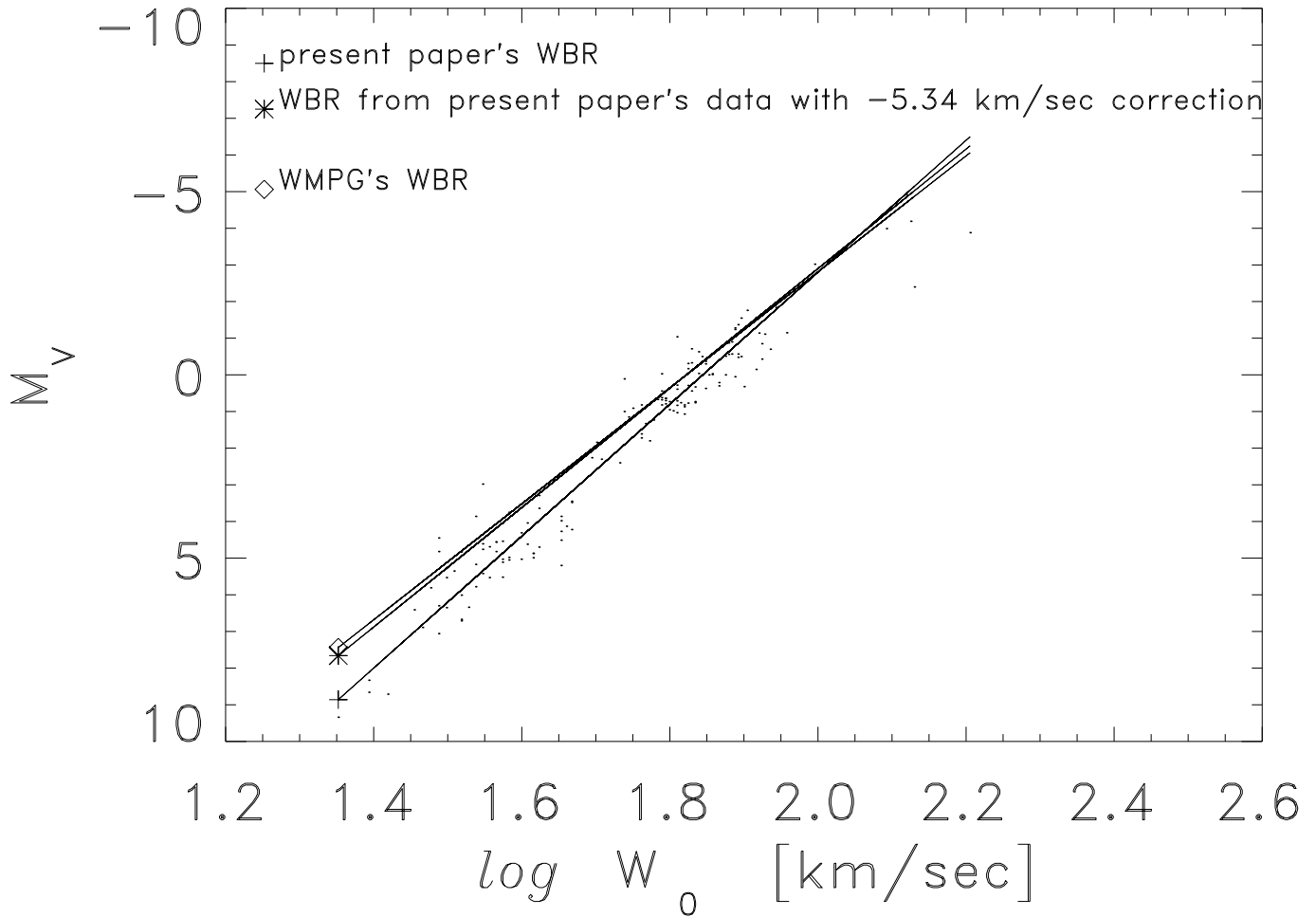


Fig. 6. Comparison between the following calibrations: the present paper's one ($M_V = 33.2 - 18.0 \cdot \log W_0$), the one we obtained after subtracting $5.34 \text{ km} \cdot \text{s}^{-1}$ to all W_0 measurements and that of WMPG (the weighted one: $M_V = 28.83 - 15.82 \cdot \log W_0$). The points refer to our data, including stars not used in the calibration because of the uncertainty in the parallax ($\frac{\sigma_\pi}{\pi} > 0.1$) or because they are binary or multiple systems.

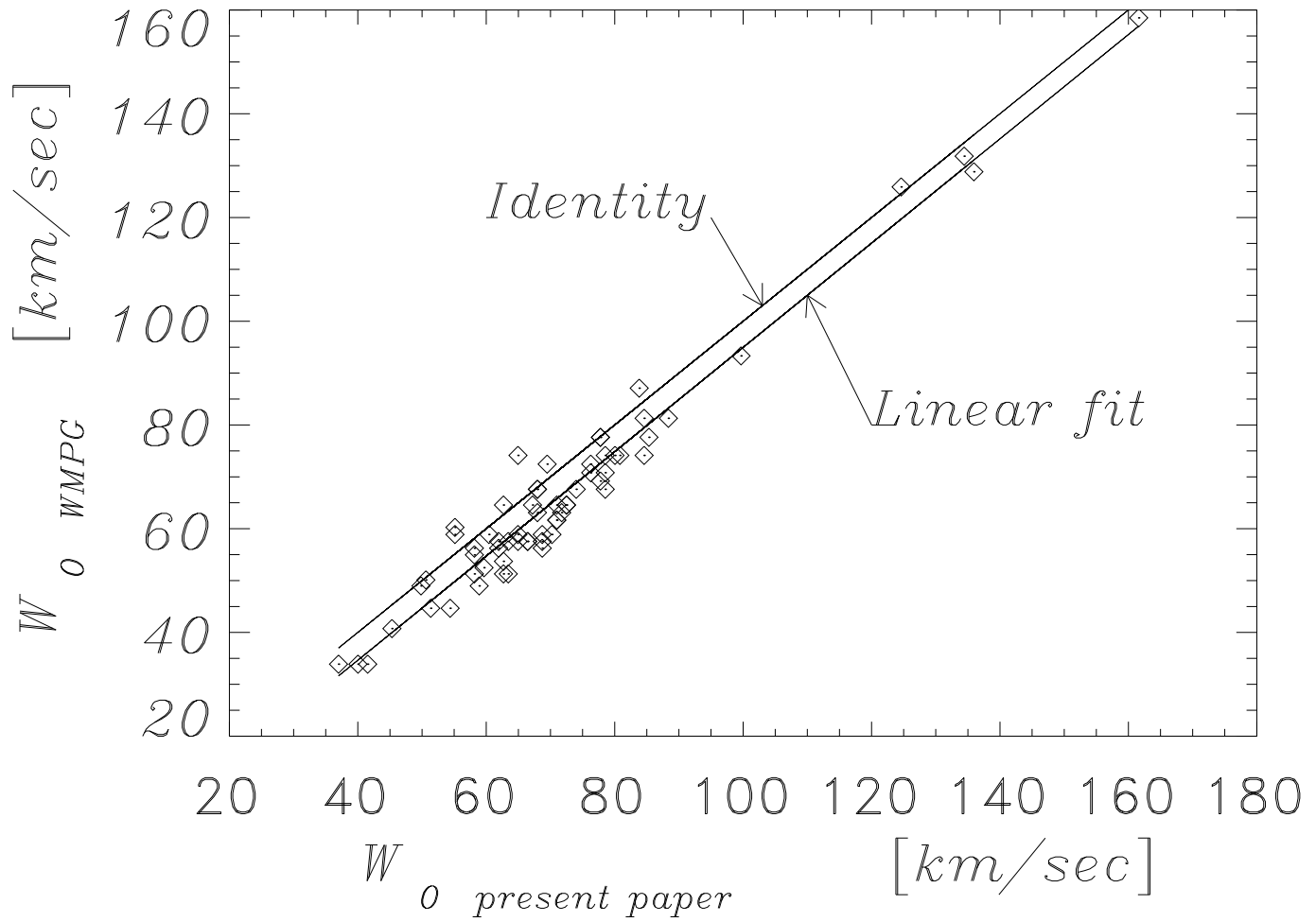


Fig. 7. Comparison between our measurements of W_0 and those used by WMPG.